

Figure 3.2 Calculated profiles of the O₃ and O number density (solid lines, bottom axis), and the ratio [O]/[O₃] (dashed line, top axis). Calculation is for 45°N equinoctial conditions based on daytime-average constituent abundances and photolysis rates.

From Andrew Dessler, *The Chemistry and Physics of Stratospheric Ozone*, San Diego, CA: Academic Press, 2000.

Key Atmospheric Data

TABLE A.8 U.S. Standard Atmosphere, 1976

Height, km	Pressure, hPa	Temperature, K	Density, g m ⁻³	Water Vapor	
				Moist Stratosphere, g m ⁻³	Dry Stratosphere, g m ⁻³
0	1.013×10^3	288	1.225×10^3	5.9	5.9
1	8.98×10^2	282	1.112×10^3	4.2	4.2
2	7.950×10^2	275	1.007×10^3	2.9	2.9
3	7.012×10^2	269	9.093×10^2	1.8	1.8
4	6.166×10^2	262	8.194×10^2	1.1	1.1
5	5.405×10^2	256	7.364×10^2	6.4×10^{-1}	6.4×10^{-1}
6	4.722×10^2	249	6.601×10^2	3.8×10^{-1}	3.8×10^{-1}
7	4.111×10^2	243	5.900×10^2	2.1×10^{-1}	2.1×10^{-1}
8	3.565×10^2	236	5.258×10^2	1.2×10^{-1}	1.2×10^{-1}
9	3.080×10^2	230	4.671×10^2	4.6×10^{-2}	4.6×10^{-2}
10	2.650×10^2	223	4.135×10^2	1.8×10^{-2}	1.8×10^{-2}
11	2.270×10^2	217	3.648×10^2	8.2×10^{-3}	8.2×10^{-3}
12	1.940×10^2	217	3.119×10^2	3.7×10^{-3}	3.7×10^{-3}
13	1.658×10^2	217	2.666×10^2	1.8×10^{-3}	1.8×10^{-3}
14	1.417×10^2	217	2.279×10^2	8.4×10^{-4}	8.4×10^{-4}
15	1.211×10^2	217	1.948×10^2	7.2×10^{-4}	7.2×10^{-4}
16	1.035×10^2	217	1.665×10^2	5.5×10^{-4}	3.3×10^{-4}
17	8.850×10^1	217	1.423×10^2	4.7×10^{-4}	2.8×10^{-4}
18	7.565×10^1	217	1.217×10^2	4.0×10^{-4}	2.4×10^{-4}
19	6.467×10^1	217	1.040×10^2	4.1×10^{-4}	2.1×10^{-4}
20	5.529×10^1	217	8.891×10^1	4.0×10^{-4}	1.8×10^{-4}
21	4.729×10^1	218	7.572×10^1	4.4×10^{-4}	1.5×10^{-4}
22	4.048×10^1	219	6.450×10^1	4.6×10^{-4}	1.3×10^{-4}
23	3.467×10^1	220	5.501×10^1	5.2×10^{-4}	1.1×10^{-4}
24	2.972×10^1	221	4.694×10^1	5.4×10^{-4}	9.4×10^{-5}
25	2.549×10^1	222	4.008×10^1	6.1×10^{-4}	8.0×10^{-5}
30	1.197×10^1	227	1.841×10^1	3.2×10^{-4}	3.7×10^{-5}
35	5.746	237	8.463	1.3×10^{-4}	1.7×10^{-5}
40	2.871	253	3.996	4.8×10^{-5}	7.9×10^{-6}
45	1.491	264	1.966	2.2×10^{-5}	3.9×10^{-6}
50	7.978×10^{-1}	271	1.027	7.8×10^{-6}	2.1×10^{-6}
70	5.220×10^{-2}	220	8.283×10^{-2}	1.2×10^{-7}	1.8×10^{-7}
100	3.008×10^{-4}	210	4.990×10^{-4}	3.0×10^{-4}	1.0×10^{-9}

From John H. Seinfeld and Spyros N. Pandis, *Atmospheric Chemistry and Physics*, Hoboken, NJ: John Wiley & Sons, 2006.

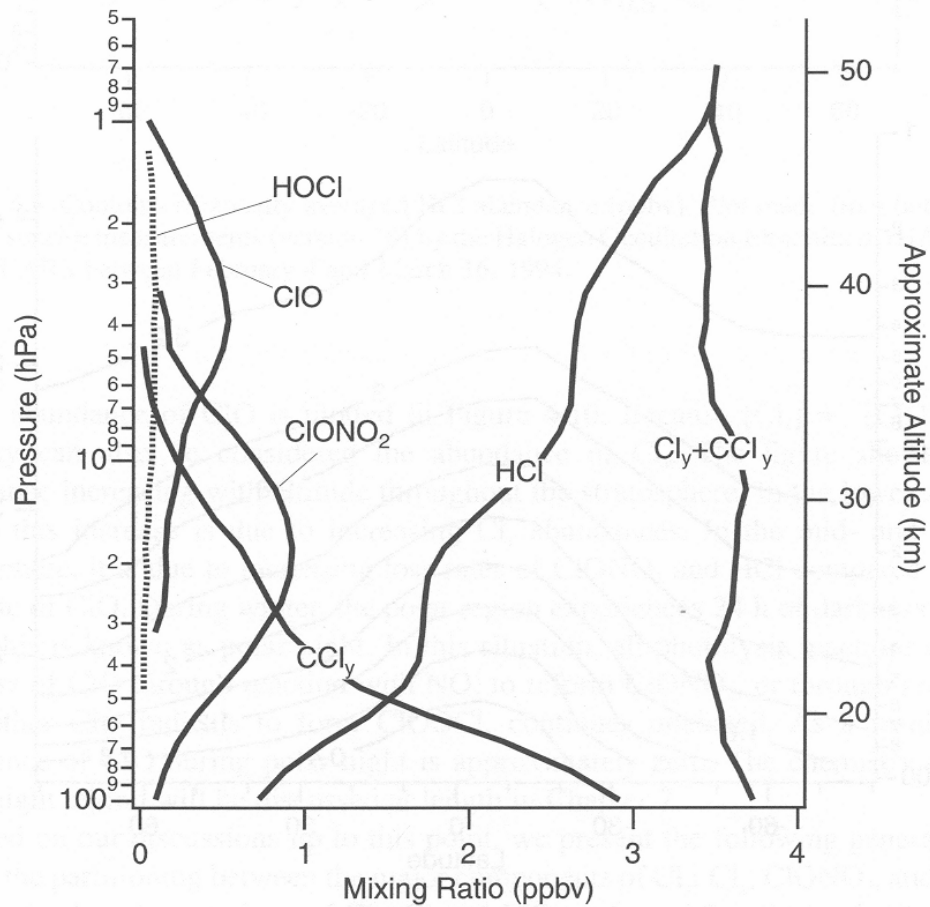


Figure 4.6 Measurements of the major components of stratospheric chlorine versus pressure. Data were measured in November 1994 and between 20°N and 49°N [89].

From Andrew Dessler, *The Chemistry and Physics of Stratospheric Ozone*, San Diego, CA: Academic Press, 2000.

ONATURE

NATURE VOL. 315 16 MAY 1985

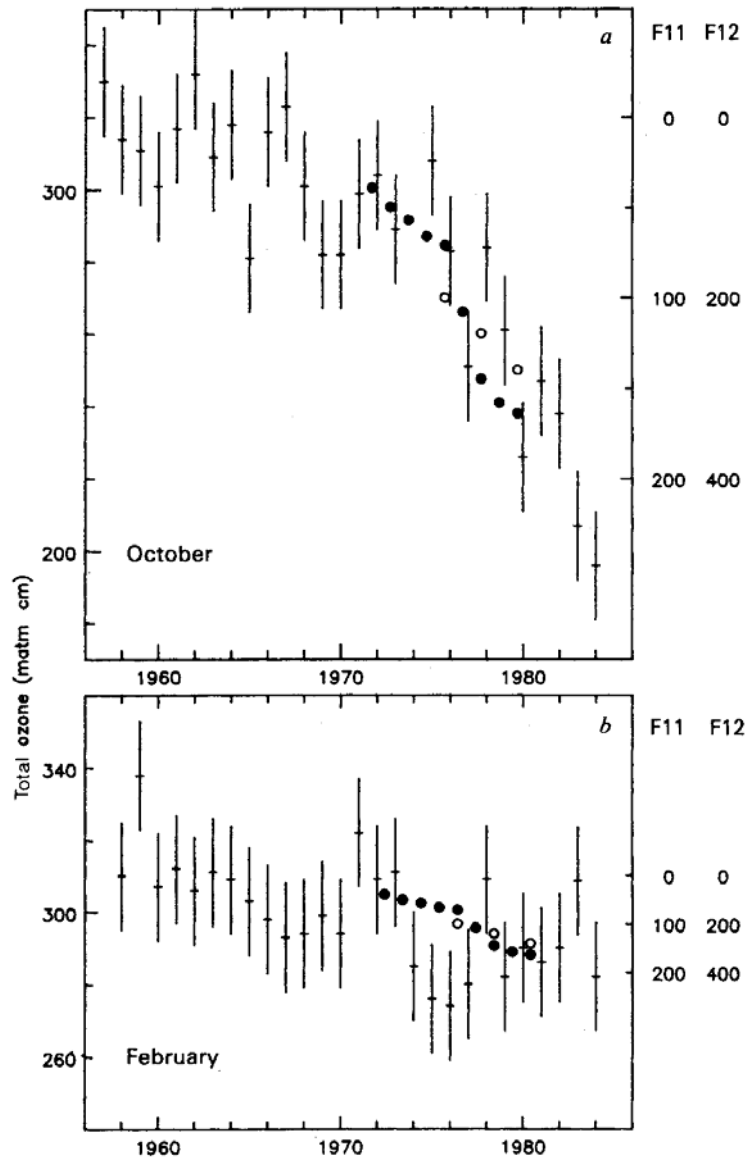


Fig. 2 Monthly means of total O_3 at Halley Bay, and Southern Hemisphere measurements of F-11 (\bullet , p.p.t.v. (parts per thousand by volume) $CFCl_3$) and F-12 (\circ , p.p.t.v. CF_2Cl_2). *a*, October, 1957-84. *b*, February, 1958-84. Note that F-11 and F-12 amounts increase down the figure.

Farman, J. C.; Gardiner, B.G.; Shanklin, J. D, *Nature* **1985**, 315, 207-210.

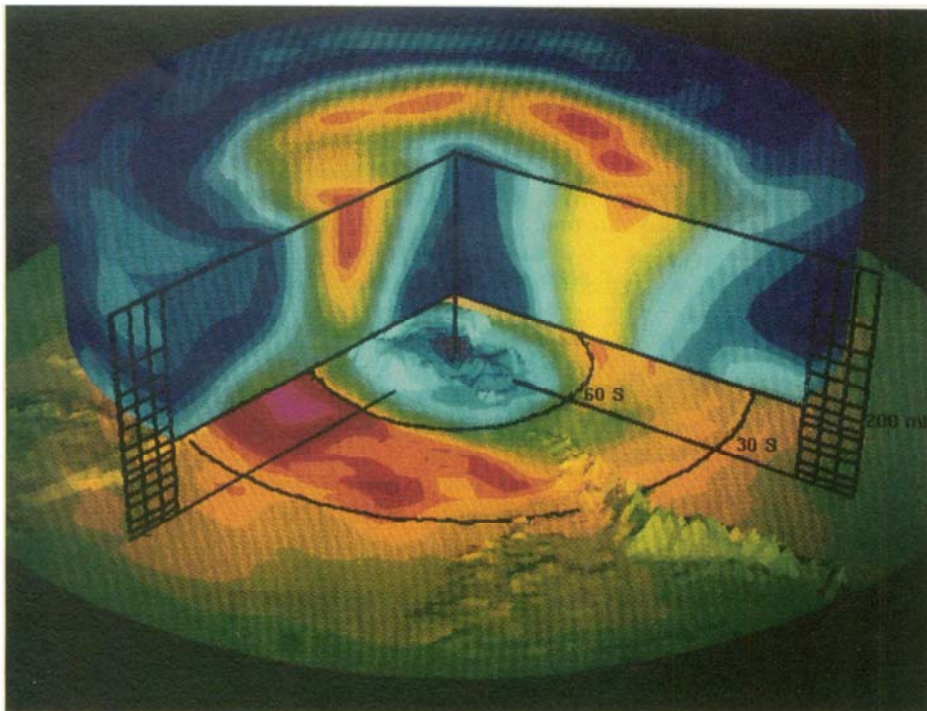


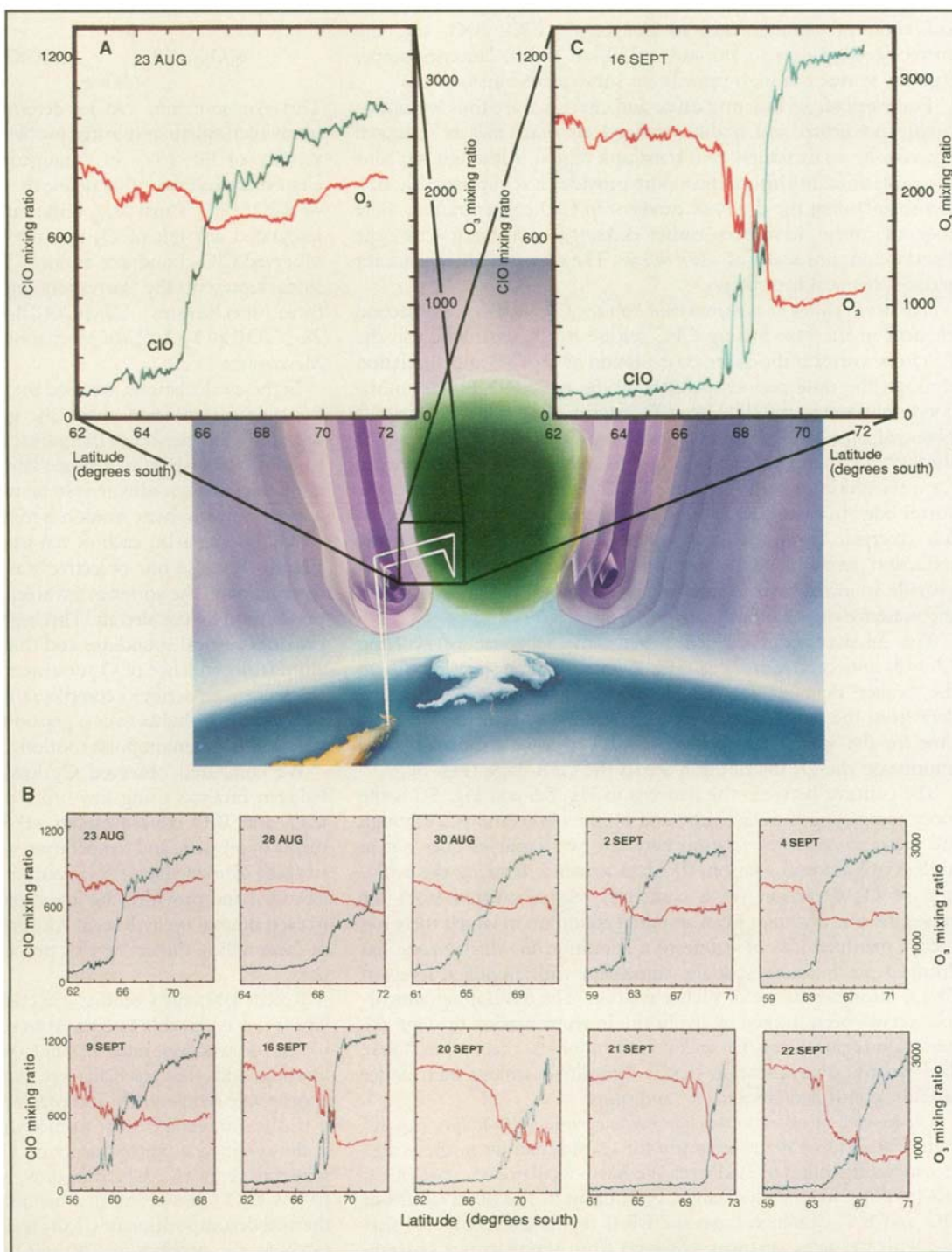
Fig. 1. The Antarctic polar vortex and the ozone hole on 7 October 1989. Upper part of the figure (cylindrical structure with missing wedge) shows the wind speeds. Wind speeds range from 0 (dark blue) to 80 m s^{-1} (red); the cylinder is centered on the south pole. Surface plot below shows the orography not to scale; the Andes are the chain of mountains moving from the center of the figure to the lower right, Antarctica is at the center, and southern Africa is on the left. The surface color scheme shows total ozone, and blue colors indicate values below 200 Dobson Units (DU). Grids indicate standard pressure levels; the wind speed plot starts at 200 mb (10 km) and extends to 10 mb (30 km). Latitudes are shown at 30° and 60° . The figure shows the containment of the ozone hole by the strong wind belt or polar vortex.

Schoeberl, Mark R.; Hartmann, Dennis L. *Science* **1991**, *251*, 46-52.

Free Radicals Within the Antarctic Vortex: The Role of CFCs in Antarctic Ozone Loss

J. G. ANDERSON, D. W. TOOHEY, W. H. BRUNE

Science 1991, 251, 39-46.



Protonation of Chlorine Nitrate and Nitric Acid: Identification of Isomers by Vibrational Spectroscopy

Jong-Ho Choi,[†] Keith T. Kuwata, Yi-Bin Cao, Bernd-Michael Haas,[‡] and Mitchio Okumura^{*}

Arthur Amos Noyes Laboratory of Chemical Physics, California Institute of Technology, Pasadena, California 91125

Received: February 28, 1997; In Final Form: May 14, 1997[⊗]

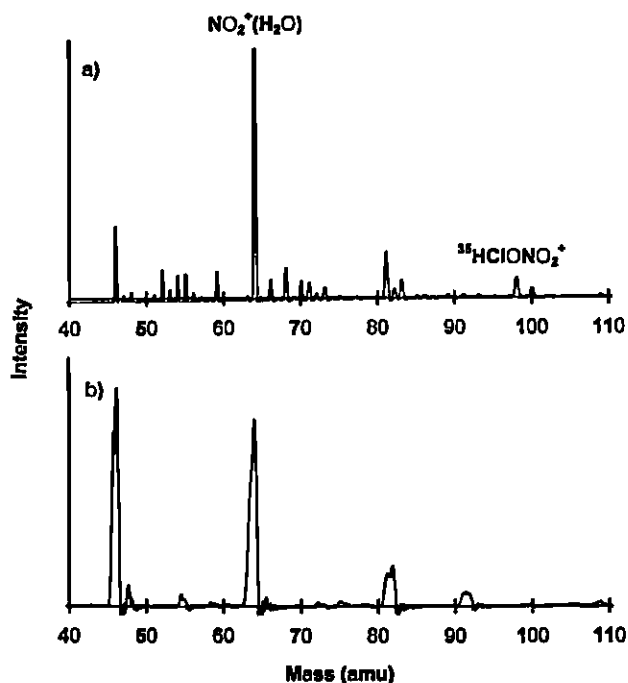


Figure 3. Time-of-flight mass spectra of chlorine nitrate seeded in H_2 , ionized (a) by an electron beam and (b) in a glow discharge. Protonated chlorine nitrate, $HClONO_2^+$, is seen only in spectrum a. The two chlorine isotopomers can be seen at $m/e = 98$ and 100 .

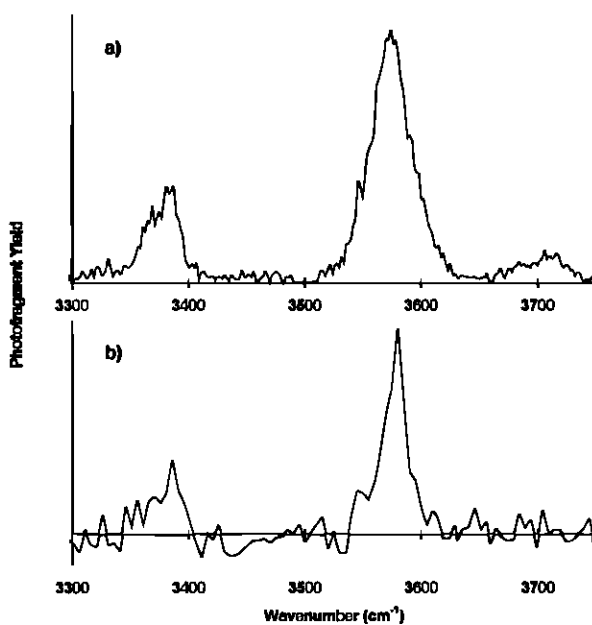
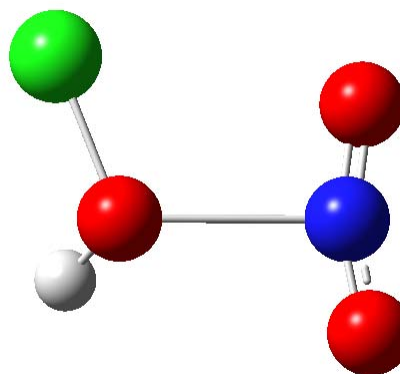


Figure 6. Vibrational predissociation spectra of the two isotopomers of protonated chlorine nitrate, $HClONO_2^+$, formed by electron beam ionization of the free jet expansion. Spectra were recorded for parent ions of (a) $m/e = 98$ and (b) $m/e = 100$.

Reaction of Chloride Ions with Chlorine Nitrate and Its Implications for Stratospheric Chemistry

Bernd-Michael Haas, Kevin C. Crellin, Keith T. Kuwata, and Mitchio Okumura*

Arthur Amos Noyes Laboratory of Chemical Physics,† California Institute of Technology, Pasadena, California 91125

Received: February 16, 1994; In Final Form: May 3, 1994*

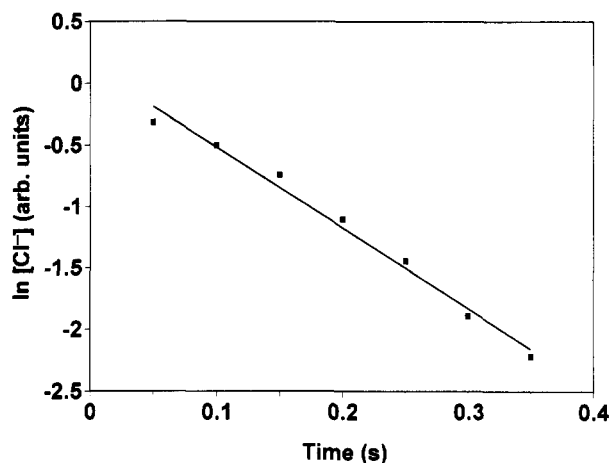


Figure 2. Observed decay of the Cl^- abundance with time for a single run. The line is a fit to the data. Conditions were the same as in Figure 1.

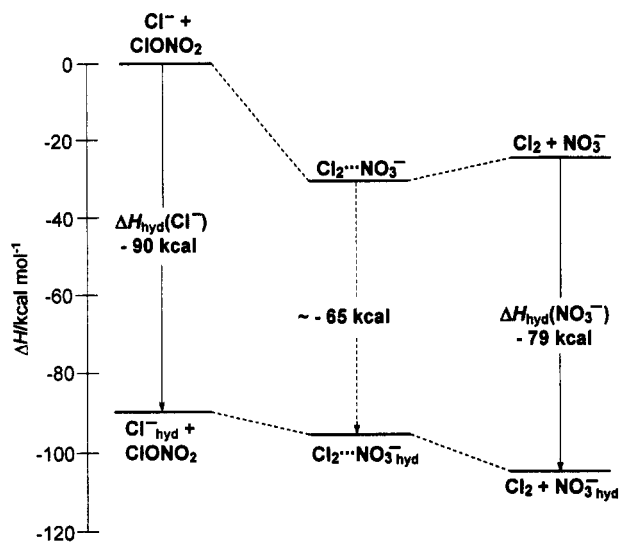
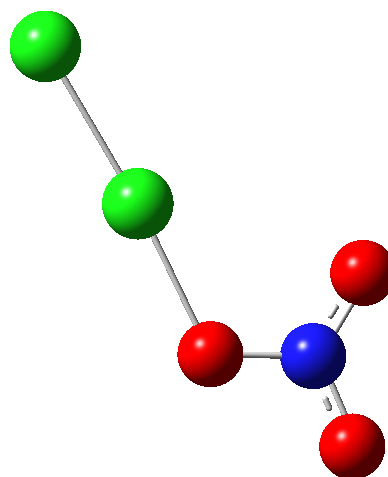


Figure 4. Reaction coordinate diagram for $\text{Cl}^- + \text{ClONO}_2 \rightarrow \text{Cl}_2 + \text{NO}_3^-$. The upper curve is based on the gas-phase enthalpies. The lower curve includes corrections for ion solvation enthalpies. The ionic hydration enthalpy of the $\text{Cl}_2 \cdots \text{NO}_3^-$ intermediate is obtained from an estimate of the hydration of the *ab initio* charge distribution (see text).